

Case Study: Traveling-Wave Fault Locating for an HVdc Transmission Line

Diogo Totti and Samuel Lacerda
Interligação Elétrica do Madeira S/A

Paulo Lima, Venkat Mynam, and Ricardo Abboud
Schweitzer Engineering Laboratories, Inc.

Presented at the
50th Annual Western Protective Relay Conference
Spokane, Washington
October 10–12, 2023

Case Study: Traveling-Wave Fault Locating for an HVdc Transmission Line

Diogo Totti and Samuel Lacerda, *Interligação Elétrica do Madeira S/A*
 Paulo Lima, Venkat Mynam, and Ricardo Abboud, *Schweitzer Engineering Laboratories, Inc.*

Abstract—This paper presents how a traveling-wave fault-locating device originally designed for ac systems can be applied in an HVdc transmission line to provide accurate fault location. The proposed scheme uses high-resolution, time-synchronized transient records to calculate the fault location. Additionally, a system for automatic fault location calculation is proposed. The paper presents validation testing performed on the instrument transformer used to measure the traveling-wave signal from the HVdc system and the fault location results for staged and real faults.

I. INTRODUCTION

Energy market deregulation in different parts of the world has changed the way transmission grid companies (TGCs) manage and operate their assets, by imposing stricter and more rigorous performance requirements. In such deregulated markets, like the Brazilian market, the earnings of TGCs are based on the amount of time the assets are made available to carry power over the bulk transmission system, not on the amount of energy that is transmitted. In the case of a transmission line, earnings are related to the amount of time that the line is in service. Financial penalties are applied when the transmission line is unexpectedly taken out of service, such as due to a permanent fault.

Due to the geographical size of the Brazilian territory, power transmission lines over very long distances have been required to meet the load demand given the location of generating plants. HVdc transmission lines are normally chosen to transport electric power over long distances and to connect power systems that operate asynchronously. The amount of energy transported by these lines is enormous and the TGC's monthly revenue relies on their availability, making accurate fault location for these HVdc transmission lines even more critical.

One such interconnection is the connection of the Madeira River Complex to the Brazilian southeast region. The Madeira River Complex is made up of two hydroelectric power plants: Jirau (3,300 MW) and Santo Antonio (3,150 MW). The southeast region is about 2,400 km from the power plants. Hence, to provide a reliable connection, two line commutated converter (LCC) bipolar HVdc lines (bipole), ± 600 kV, 2,400 km long, with 3,150 MW rated power have been used. The interconnection consists of Bipoles 1 and 2 and is one of the most important transmission corridors in the Brazilian interconnected power grid.

Fig. 1 introduces the main characteristics of Bipole 2, which is the focus of the case study in this paper. For simplicity, disconnect switches and the configuration and apparatus of

500 kV ac harmonic filters and 500 kV ac substations are not shown.

Bipole 2 has the flexibility to operate in the following modes:

- Balanced bipole mode (BPB), which is the normal operating mode.
- Unbalanced bipole mode (BPU), triggered after a dc line fault when a pole recovers with reduced voltage.
- One-pole mode with metallic return, used to avoid current flowing through earth electrodes.
- One-pole mode with ground return, which is typically triggered when a pole trips or is manually blocked.
- Reduced voltage operation at 0.7 pu dc voltage.
- High MVar consumption to support ac voltage control.

Traveling-wave fault-locating (TWFL) devices provide fault location by measuring the arrival times at the line terminal(s) of transients launched by the voltage step change due to line faults. For ac transmission line applications, conventional current transformers (CTs), inductive voltage transformers, and coupling capacitor voltage transformers designed for protection and control purposes can share the secondary ac signal with TWFL devices. Some designs incorporate the TWFL feature in a protection and control device, eliminating the need for additional equipment [1] [2].

Protection and control systems use current and voltage transducers. The accuracy of measurements taken from dc current transducers can reach the order of 0.2 percent over a very wide frequency range, similar to that of dc voltage dividers. Therefore, very accurate voltage and current signals are available even during transient conditions, allowing these signals to be used for traveling-wave-based fault location and protection.

Section II briefly reviews the TWFL system applied in ac systems in terms of design and signal processing implementation to extract highly accurate TW arrival times from the line current signal. The proposed TWFL scheme for the HVdc line uses high-resolution, time-synchronized transient records from both terminals of the line to calculate the fault location. Off-the-shelf software with tools such as the Bewley lattice diagram is used for this purpose. In addition, the paper proposes an automatic system for TWFL for HVdc lines.

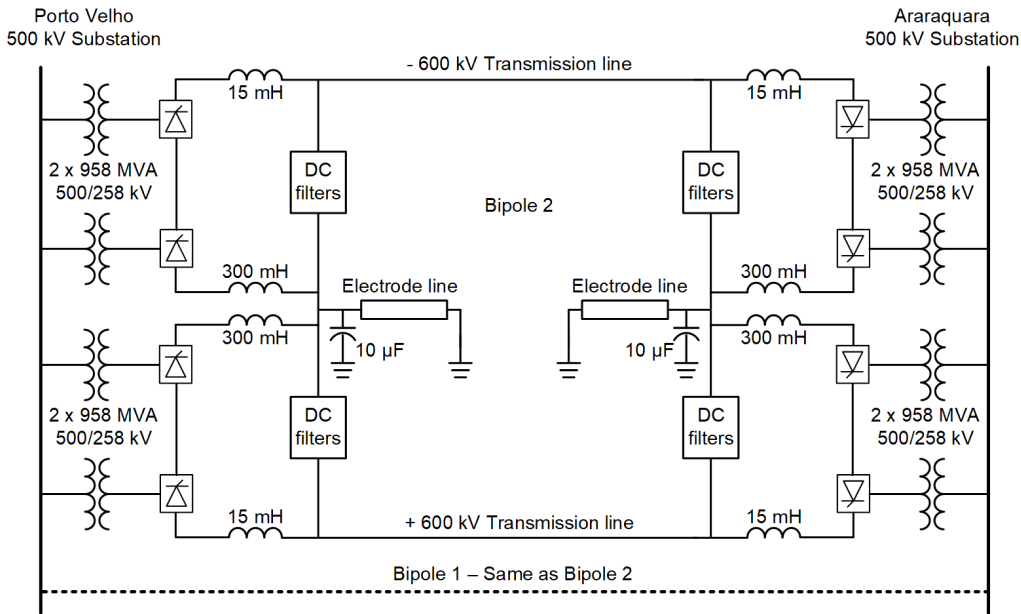


Fig. 1. Porto Velho—Araraquara LCC-HVdc bipoles, with detailed components for Bipole 2.

II. TWFL METHODS REVIEW

Power system faults cause step changes in voltage and current signals, which are referred to as traveling waves (TWs). These step changes originate at the fault location and propagate away from it. Devices with TW-based functions, including fault locating and line monitoring and protection, measure these step changes and use them to provide accurate fault location and ultra-high-speed (UHS) protection. Devices [1] [2] with these functions are successfully applied on ac systems [3]. Fig. 2 shows the voltages and currents recorded by the TW device during a fault on a 345 kV ac transmission line. The device issued the trip command based on a TW differential scheme (TW87) in less than 2.5 ms, and the fault cleared in less than 25 ms. For ac system applications, the fundamental signal needs to be filtered to extract the step changes. In Fig. 3, a differentiator-smoother filter is used to detect the TWs [4] [5].

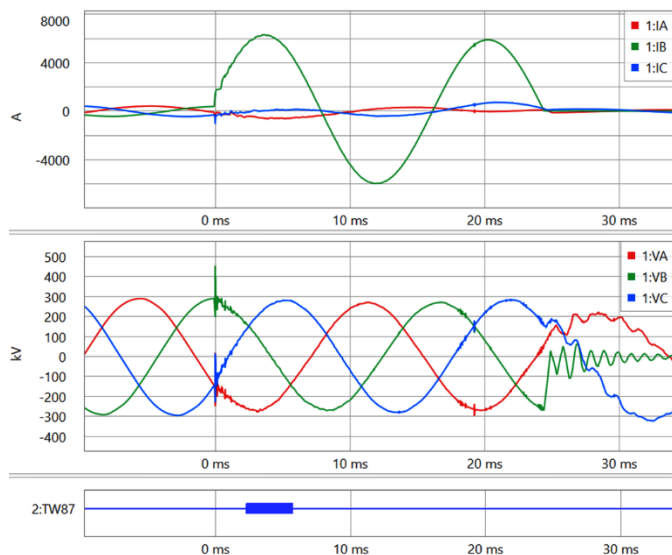


Fig. 2. Current signals show the step change distinctly at $t = 0$ ms.

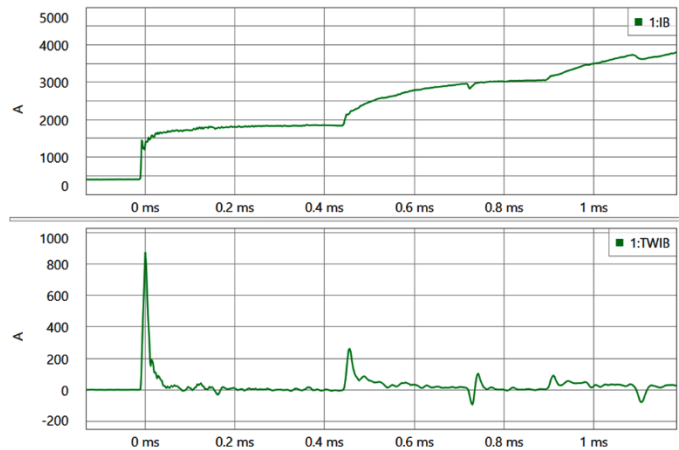


Fig. 3. A differentiator-smoother filter detects the fundamental signal preserving the step change(s).

TW functions use the magnitude, polarity, or time stamp associated with the peaks of the TWs (differentiator-smoother filter output), or a combination thereof, to calculate the required operating quantities. Interpolation techniques are used to achieve better resolution of the TW time stamp, which leads to better accuracy of the fault-locating functions [4] [5]. This paper discusses applying a TW device designed for locating faults on ac applications to an HVdc line. The dc-coupled voltage input, with 280 V peak analog-to-digital converter measurement capability combined with 1 MHz sampling rate (18 bits of resolution) recording capability, makes the application to an HVdc line feasible. Section V shows fault location errors of less than 350 m for staged and real faults in the HVdc system, as shown in Fig. 1.

A. Double-Ended Traveling-Wave-Based Fault Locating (DETWFL)

Fig. 4 shows a Bewley diagram, which is a time-spatial chart that shows TWs progressing along the time axis (down the vertical lines) and simultaneously progressing along the distance axis (left to right and vice versa), for a fault on a transmission line, having a line length of LL , at distance M from Terminal L (local) and $LL-M$ from Terminal R (remote). At the fault inception time (t_0), the step change in the voltage launches current and voltage TWs towards both line terminals. The arrival times of the first TWs at Terminals L and R are t_L and t_R , respectively.

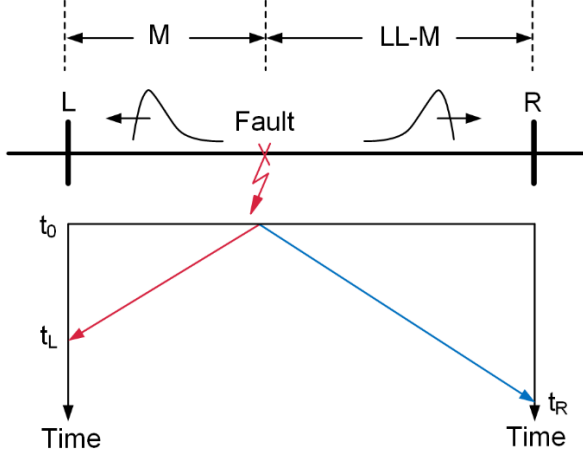


Fig. 4. The fault launches TWs that travel towards the line ends.

Devices installed at each line terminal measure TW arrival times. The DETWFL method uses the arrival time of the first TW at each terminal to calculate the fault location according to (1).

$$M = \frac{LL}{2} \left[1 + \frac{t_L - t_R}{TWLPT} \right] \quad (1)$$

where:

M is the distance to the fault location from Terminal L in kilometers or miles.

LL is the total line length in kilometers or miles.

t_L is the TW arrival time at Terminal L.

t_R is the TW arrival time at Terminal R.

$TWLPT$ is the traveling-wave line propagation time.

Real-time calculation of the DETWFL method requires device-to-device communications that allow data exchange directly between devices at each terminal [4] [5]. Alternatively, when a communications channel between devices is not available, devices at each line terminal can report the arrival time to a central device in the control center that provides the fault location [6].

In addition, the Bewley diagram tool, described in Section III, can be used to calculate the fault location.

The $TWLPT$ is the time it takes the TW to travel from one line terminal to the other. It can be measured during a transmission line energization test or using high-resolution time-synchronized transient records from both line terminals for an external event.

B. Single-Ended Traveling-Wave-Based Fault Locating (SETWFL)

The SETWFL method uses only local TW arrival times to provide the fault location. The simplified Bewley diagram for a fault on a transmission line is shown in Fig. 5. The first TW from the fault arrives at the local terminal at t_L . Part of this wave reflects and travels back to the fault; part of it is transmitted. The reflected part of the wave reflects again at the fault and arrives at the local terminal at t_{LL} .

The TW travels $2 \cdot M$ during the time interval between t_{LL} and t_L . Thus, the distance from local terminal to the fault can be estimated according to (2).

$$M = \frac{(t_{LL} - t_L) \cdot LL}{2 \cdot TWLPT} \quad (2)$$

Challenges in the implementation of SETWFL include the ability to correctly identify and measure the time stamp related to the first reflection from the fault (t_{LL} in Fig. 5) among several other TWs that could arrive in the local terminal due to reflections at the remote terminal. A TW arrived at t_{RL} in Fig. 5 (reflections from adjacent transmission lines are not shown). Reference [7] presents an innovative methodology to implement SETWFL.

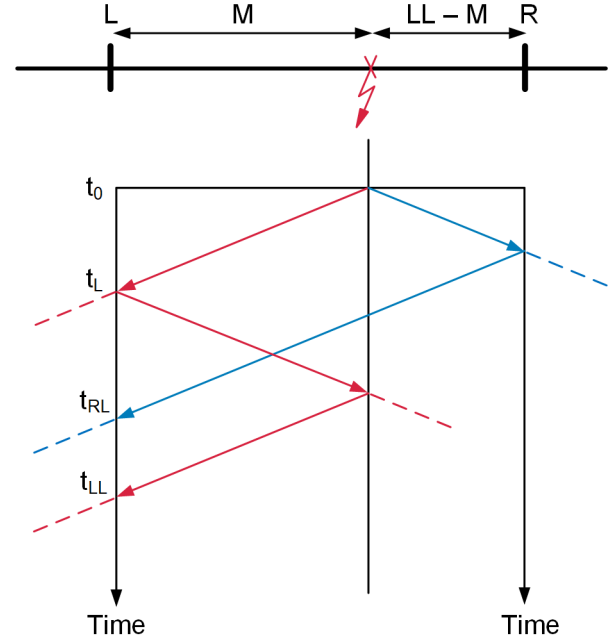


Fig. 5. A Bewley diagram illustrating the SETWFL method.

III. SOFTWARE TOOL TO CALCULATE TRAVELING-WAVE FAULT LOCATIONS

The Bewley diagram is a powerful tool to visualize and analyze TWs for fault location purposes. Reference [8] presents an offline fine tuning of the fault location using the Bewley diagram tool available in fault record event analysis software.

Fig. 6 shows TWs that arrive at each terminal for a transmission line due to a fault at Location M from Terminal L. The time-stamp label notation of each TW, proposed in [8], represents the order of the initial TW and its subsequent reflections recorded at each line terminal.

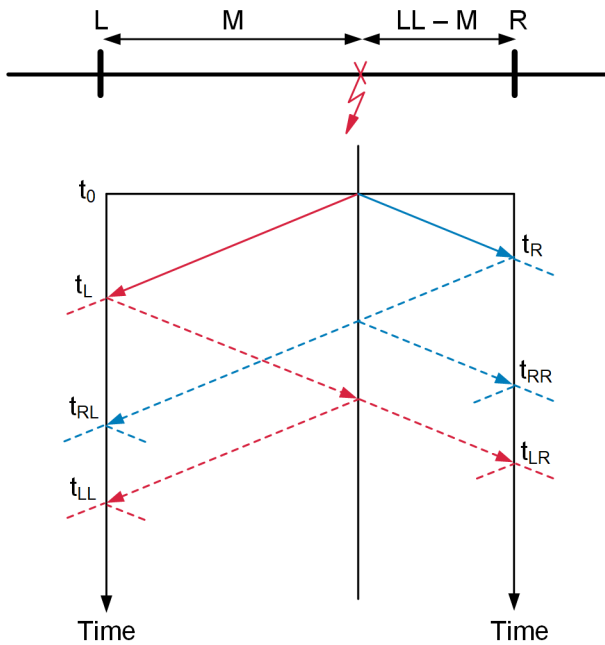


Fig. 6. A Bewley diagram with TW paths for a fault in a two-terminal transmission line.

The Bewley diagram tool [8], including time cursors, allows the user to correlate the recorded TWs with Bewley diagram arrival times for fault-locating analysis purposes. Fig. 7 shows TWs recorded at both terminals for a simulated fault in an ac transmission line 127.65 km long. The green dashed lines are the movable time cursors. Additional information, such as LL, the fault location from both terminals, the first TW arrival time, TWLPT, the traveling velocity relative to the speed of light (LPVEL), and CT cable delay compensation quantities, is shown on the left of Fig. 7.

As reviewed in Section III, the DETWFL and SETWFL methods require a pair of arrival times to estimate the fault location, (t_L , t_R) and (t_L , t_{LL}), respectively. This pair of arrival times results in a set of two equations and two unknowns, (t_0 , M). TWLPT is a predefined constant. Software allows fine tuning of the fault location result, which is achieved by providing wave arrival times associated with additional reflections.

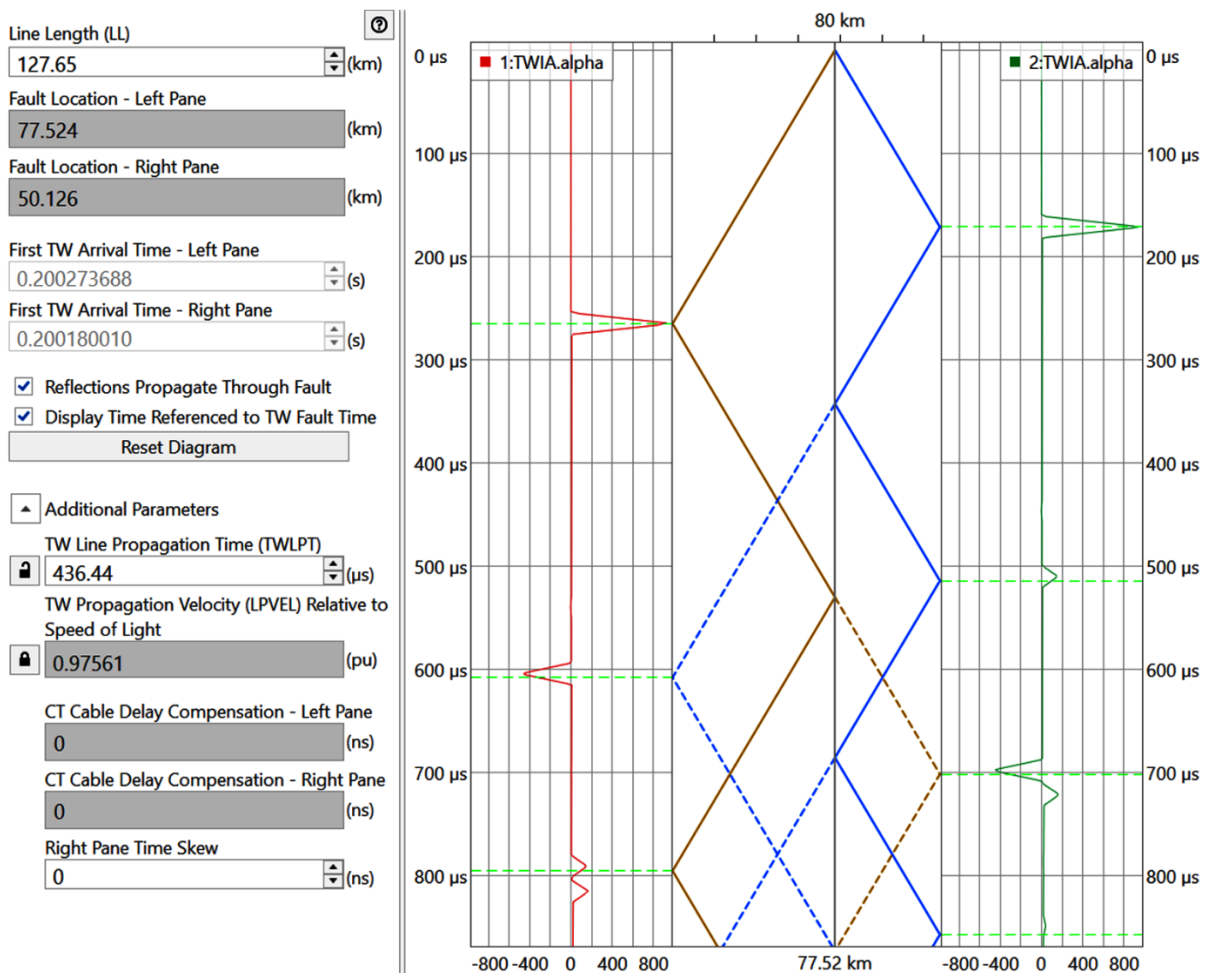


Fig. 7. Software with the Bewley diagram tool.

IV. CASE STUDY

Interligação Elétrica do Madeira (IE Madeira) is responsible for the maintenance and operation of Bipole 2, which connects the Madeira River Complex to the Brazilian southeast region, as presented in Section I.

Presently, this bipole is monitored by a traveling-wave-based fault-locating system that has been in operation for the last ten years. IE Madeira engineers are facing challenges in operating this system, including the unavailability of data for postevent analysis, failing units, and long lead times associated with spare parts. For this reason, IE Madeira engineers decided to look for an alternative solution.

IE Madeira engineers investigated TWFL solutions that could be applied to the HVdc bipole. They selected a particular solution that is available for ac systems to experiment with in their HVdc system,

This section describes the existing TWFL system used by IE Madeira, referred to as a Line Fault Locator (LFL) in this paper, and its limitations. Additionally, a pilot project using a device originally designed for ac systems to measure voltage TWs in the HVdc system is presented, including validation testing of sensors and field results.

A. LFL System Currently Operating in IE Madeira HVdc Bipole 2

Fig. 8 shows the existing LFL system and its components. The system operation and the role played by each component is described following.

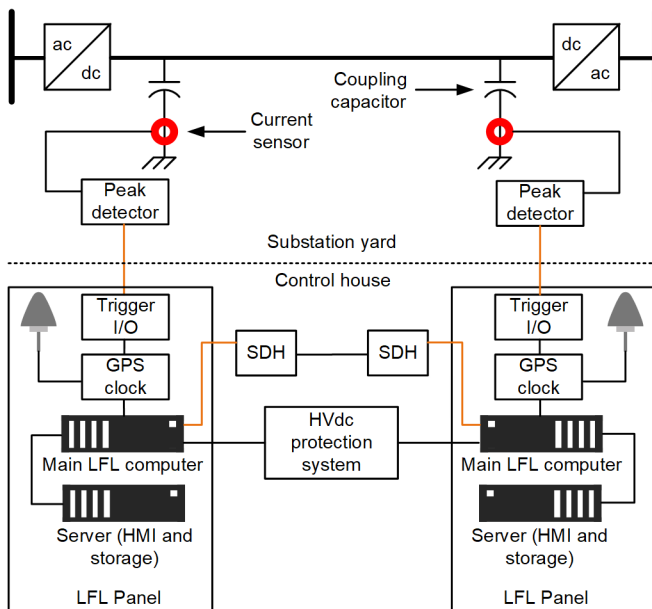


Fig. 8. Existing LFL system and components.

The coupling capacitor installed at each HVdc pole terminal is 10 meters tall and has a capacitance of 2,900 pF. Fig. 9 shows the capacitor coupling at Araraquara Substation, which is located after the dc filter represented in Fig. 1, near the first transmission line tower. The only application for this capacitor is to provide the means to measure TWs without using the sensors interfaced with the protection and control system.



Fig. 9. The coupling capacitor at Araraquara Substation.

During normal operating conditions, the voltage at the capacitor terminal is constant and the current through it is zero. A fault in the HVdc line causes a step change in the dc voltage, resulting in transient current through the capacitor according to (3).

$$I_c = C \cdot \frac{dv(t)}{dt} \quad (3)$$

where:

I_c is the current through the coupling capacitor.

C is coupling capacitor capacitance.

$v(t)$ is the voltage drop across the capacitor.

The current sensor shown in Fig. 10 is capable of measuring current signals at frequencies ranging from 0.5 Hz to 500 MHz. The output signal of the sensor is an accurate voltage signal representing the measured current. The output voltage is proportional to the input current, with a ratio of 10:1. The maximum peak current is 10,000 A.



Fig. 10. The current sensor.

The peak detector, shown in Fig. 8, sends an optical pulse when the voltage signal exceeds an adjusted level. This level is set to 3 V, meaning that a minimum of 10.3 kV/ μ s is required to trigger the LFL. The current sensor and peak detector are installed in the substation yard, close to the coupling capacitor.

At the substation control house, the trigger I/O detects the optical pulse and converts it to an electrical output, which then triggers a GPS clock to get the pulse time stamp. The GPS clock provides the pulse time stamp to the main LFL computer, which

also receives the pulse time stamp from the remote terminal via the telecommunications system. With the pulse time stamps from both terminals available, the main LFL computer is capable of providing the fault location by using the DETWFL method. The HVdc protection system also provides a trigger signal to the main LFL computer to allow the fault location calculation only for internal fault conditions.

Finally, the system has a server computer that maintains the historical fault location data and has an HMI to allow operators to change settings and view fault location results.

B. LFL System Limitations

The system is in operation and has been providing fault location results with errors on the order of 1 km, which is relatively low for a 2,400 km long transmission line. The main technical limitation of the LFL is the lack of transient recording to allow fault location evaluation and troubleshooting, especially in cases where the HVdc line experiences a fault and the LFL does not provide an estimate for the fault location.

The number of components and their obsolescence is also a concern for IE Madeira, as failures in these components have led to expensive repairs. Additionally, the main LFL computer and server computer are based on an outdated and obsolete operational system, which creates cybersecurity concerns. Component obsolescence creates a challenge when hardware failures occur.

C. Pilot Project

Fig. 11 shows the pilot project TWFL system and its components.

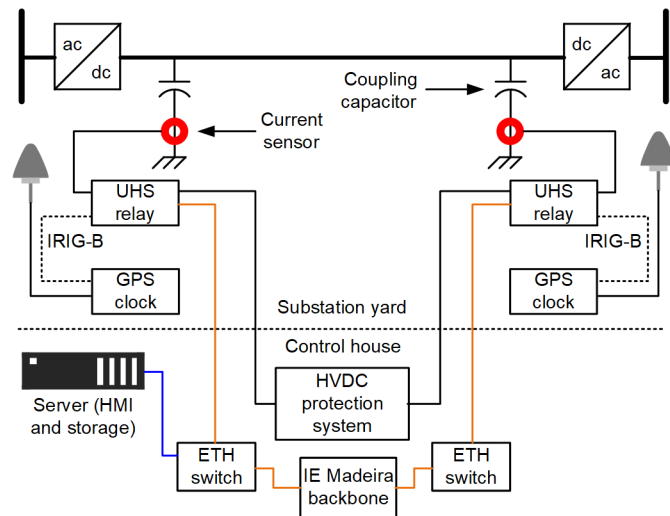


Fig. 11. Pilot project TWFL system and components.

For the pilot project, a second current sensor with the same specifications as the one described previously was installed in the positive HVdc line pole to provide the coupling capacitor current to a UHS protective relay. The sensor output voltage is wired to the UHS relay voltage input.

The capabilities of the UHS relay include time-domain line protection that uses TWs and incremental quantities, TW-based fault locating, and high-resolution oscillography (1 MHz). All functions of the UHS relay were originally designed for ac systems, thus this device is applied here only to measure and record the current sensor voltage output with accurate time-stamping to submicrosecond accuracy [1] [2].

The UHS relays have a built-in TW-disturbance detector function (TWDD), for both voltage (TWVDD) and current (TWIDD) channels, and its assertion is configured in this application to trigger the event record. Additionally, the event record is configured to trigger if the HVdc protection system operates. Event records in IEEE COMTRADE format are automatically collected from both terminals and stored in a server computer located in one of the stations. These records are available for offline fault location calculations and for further analysis.

Next in this section, we present the validation testing performed on the current sensor, an offline fault location calculation using field data from staged faults in the HVdc line, and a system capable of automatically collecting the event records, calculating the fault location, and presenting the result in a local HMI or sending it to a remote HMI.

D. Current Sensor Validation

We configured the setup shown in Fig. 12 to validate the current sensor response and its compatibility with the UHS relay voltage input.

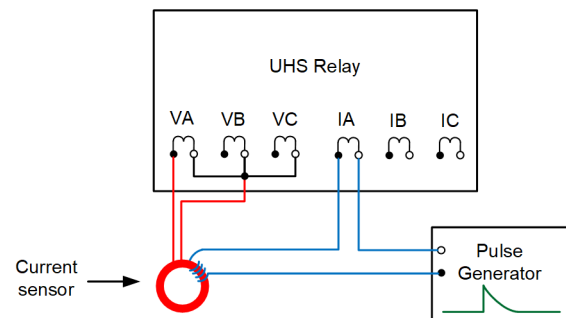


Fig. 12. Current sensor validation test setup.

The pulse generator [9] is a test set that generates a step change in current with microsecond rise time, adequately slow decay, and nanosecond precision. This pulse generator is normally used to test TW-based protection and locating devices.

In the test setup, the output of the step generator is wired through the current sensor and the UHS relay current input, IA. The output of the current sensor is wired to the voltage input of the UHS relay VAN. This setup allows us to compare the primary signal for the current sensor (IA) with its output (VAN).

Fig. 13 shows the event report from one of the tests, where the primary cable has 10 turns around the current sensor to increase the primary signal. The injected signal, IA, has a peak of approximately 4 A and the recorded voltage output has a peak value of approximately 4 V. For 40 A current input ($10 \cdot 4$ A), an output of 4 V ($40 \text{ A} \cdot 0.1 \text{ V/A}$) is expected.

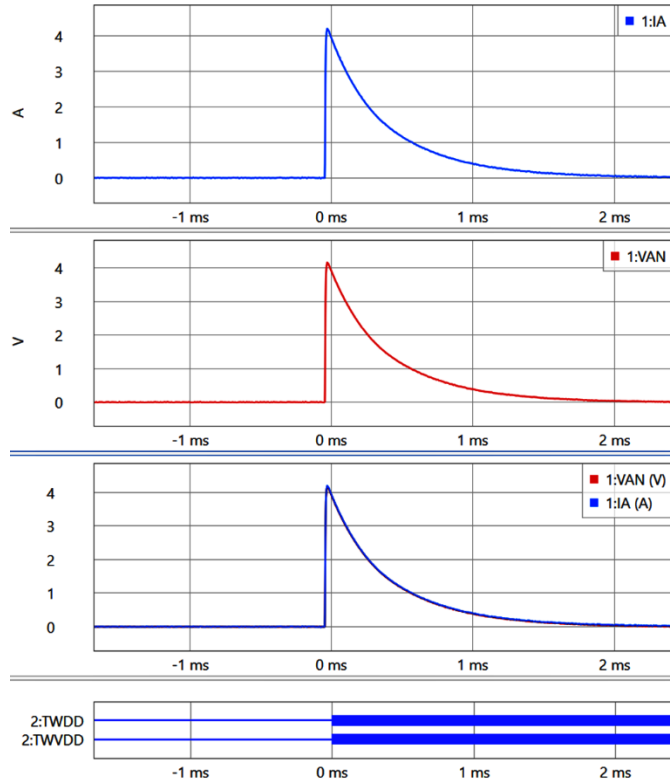


Fig. 13. Current sensor input (IA), current sensor output (VA), and voltage disturbance detector activation for a current sensor test.

In the third analog window, both the injected current (IA) and output voltage (VAN) are plotted together. VAN superimposes IA; thus, one can conclude that the current sensor does not add errors in magnitude or delay the input signal. The activation of the TWVDD and TWDD is also shown.

Fig. 14 shows the signal flow and expected shape associated with the coupling capacitor current and the current sensor output voltage signal for a step change in the HVdc voltage due to a fault. We discussed using the differentiator-smoother filter in Section II to extract the step changes. In this application, the coupling capacitor serves the role of a differentiator; therefore, the measured output voltage of the current sensor (without postprocessing with the digital differentiator-smoother filter) is used to estimate the wave arrival time.

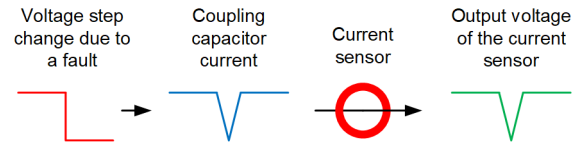


Fig. 14. The signal flow expected for an HVdc fault.

V. FIELD RESULTS

Fault location results are not available automatically by the system because the UHS relays apply current-based DETWFL and SETWFL methods. Therefore, in this section, event analysis software is used for obtaining the DETWFL results.

A. Offline Fault Location Using Field Records From Real Faults

During the pilot project period, two real faults were recorded by UHS relays.

1) Fault 1

On October 5th, 2022, there was a fault in the monitored HVdc poles. Fig. 15 shows the first TW signal recorded at each line terminal. In this paper, the sensor output voltage recorded by the UHS relay is labeled VA_ARA for the Araraquara Station and VA_CPV for the Conversora Porto Velho Station. In Fig. 15, the TW recorded at time zero is VA_CPV.

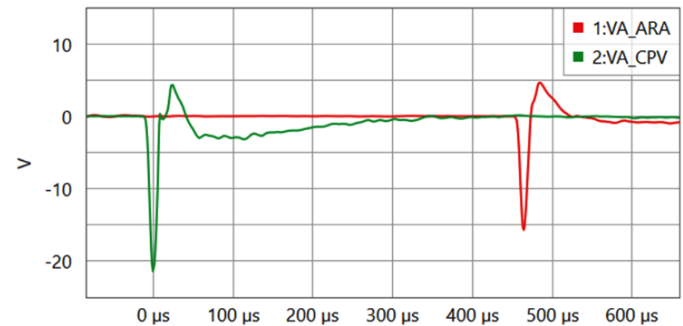


Fig. 15. Record of the initial TWs that arrived at each HVdc line terminal for Fault 1.

Using the software tool presented in Section III, the fault location can be estimated with the DETWFL method using the initial TW that arrives at each terminal. In Fig. 16, the green time cursor is pinned to the first TW that arrived at the local terminal at time t_L , and the red time cursor is pinned to the first TW that arrived at the remote terminal at time t_R . The software calculates the fault location as 1,269.166 km from Araraquara Station and 1,132.634 km from Conversora Porto Velho Station. For this calculation, the TWLPT is the default value of

8,166.12 μs —considering a default LPVEL of 0.98107 pu and the LL of 2,401.8 km, which is the length of the power conductors for Bipole 2.

CT cable delay compensation, which is the time it takes a TW to travel from the instrument transformers to the terminals of the relay, was set to zero in both terminals since the distances from the coupling capacitors to the sensors and from the sensors to the UHS relay voltage input are practically the same at both terminals.

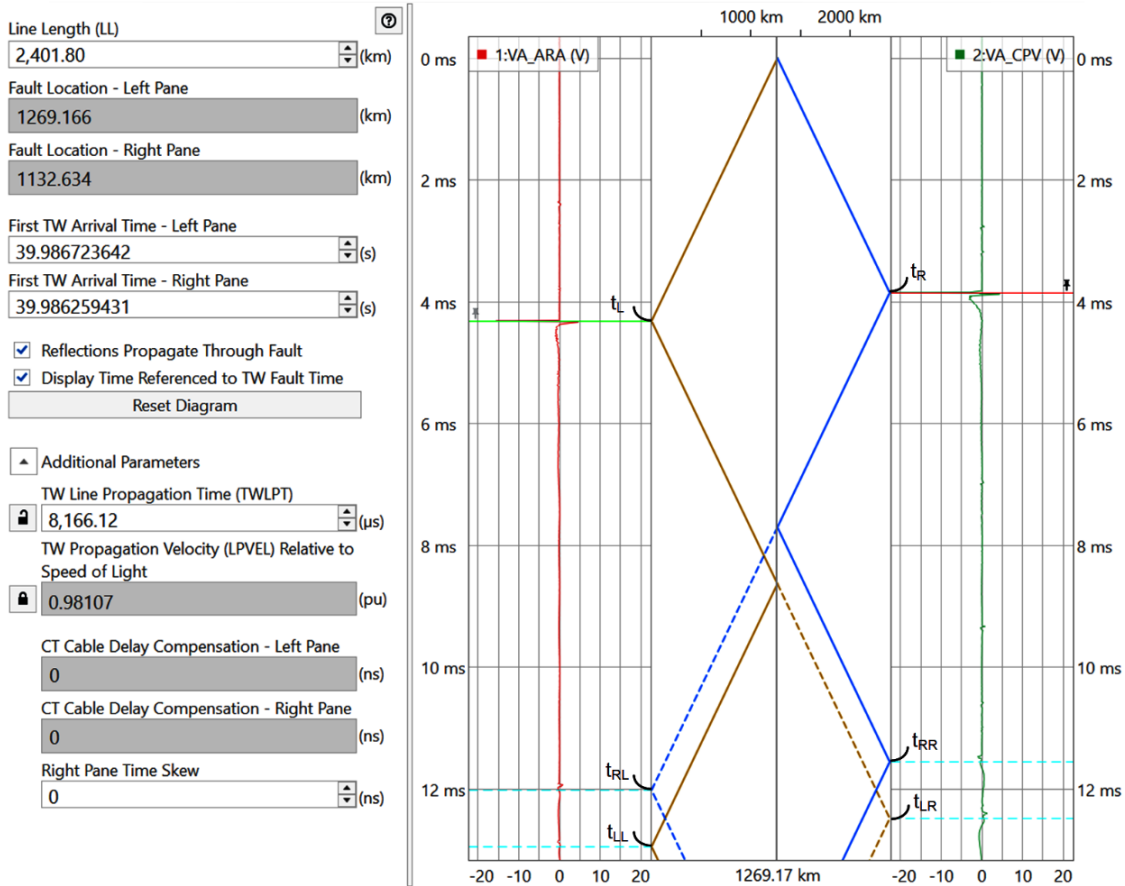


Fig. 16. The Bewley diagram and DETWFL result obtained by using two TW arrivals (t_L and t_R) to calculate the fault location for Fault 1.

As explained in [8], pinning a third cursor (blue) to the TW that arrives at t_{LL} and a fourth cursor (purple) to the TW that arrives at t_{RR} allows the software to recalculate TWLPT and the time skew (Δ), resulting in an improved fault location. The new fault location calculated is 1,269.707 km from Araraquara Station and 1,132.093 km from Conversora Porto Velho Station, as shown in Fig. 17. A new TWLPT of 8,086.88 μ s and a time skew of 848 ns is calculated by the software.

With four time cursors pinned, a better match of the time cursors can be observed related to times t_{RL} and t_{LR} to the TW peaks recorded in both terminals. For this fault, there is no confirmation of the field fault location from the line crew; however, the lightning monitoring system recorded an event at the same time and location. Additionally, the correlation of the Bewley diagram (showing expected TWs) and the recorded TWs provides confidence in the estimated fault location.

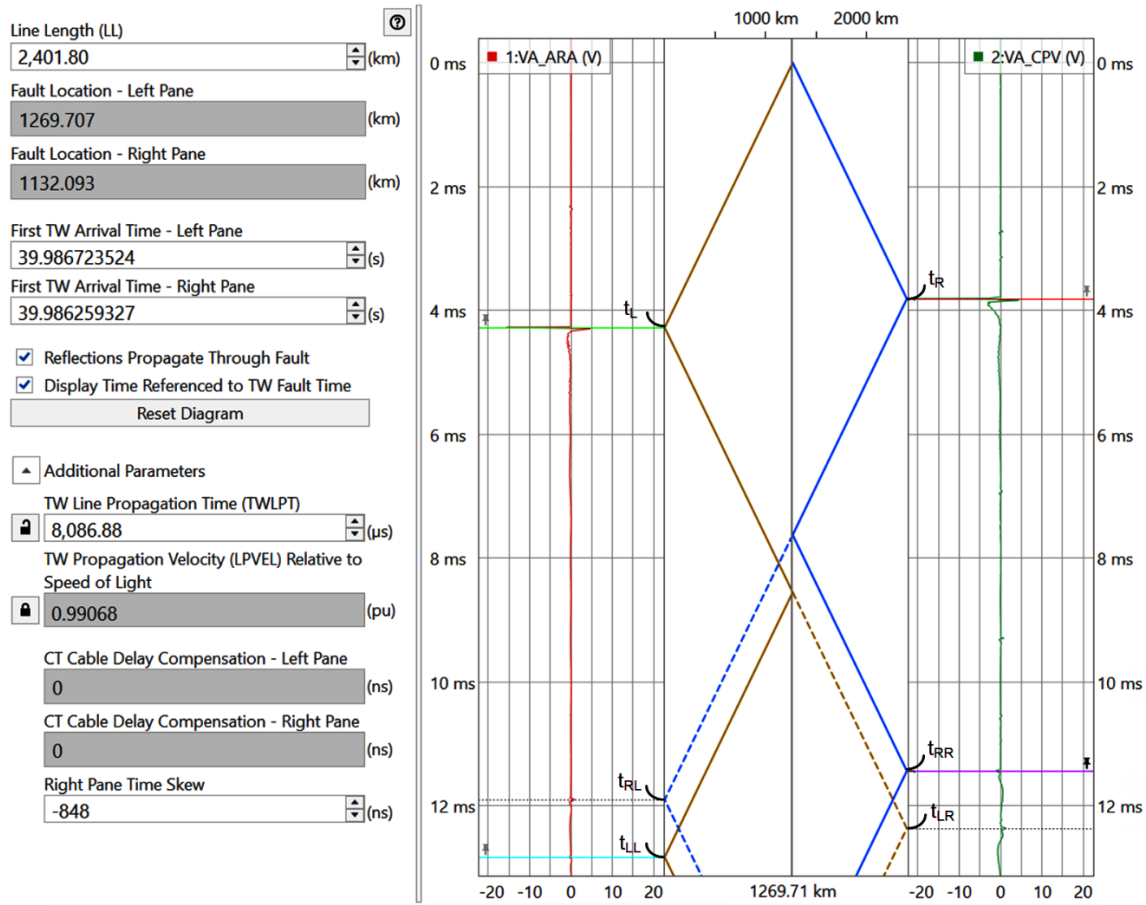


Fig. 17. The Bewley diagram and DETWFL result obtained by using a third TW arrival time (t_{LL}) and a fourth TW arrival time (t_{RR}) for improved fault location for Fault 1.

2) *Fault 2*

On July 18th, 2023, another fault triggered the fault-locating system. Fig. 18 shows the first TW signals recorded at each line terminal and a zoomed-in view of the first TWs, which activated the TWVDD and digital input related to the HVdc protection system operation (IN101) in the Araraquara Station. TWVDD and IN101 asserted at approximately 85 μ s and approximately 35 ms, respectively, after the arrival of the first TW at Araraquara Station. Fig. 18 also shows several low-magnitude TWs recorded at both terminals.

In Fig. 18, the TW recorded at time zero is VA_CPV.

Using four TW arrival times (t_L , t_R , t_{LL} and t_{RR}), Fig. 19 shows the calculated fault location of 1,238.922 km from the Araraquara Station, a TWLPT of 8,081.30 μ s and a time skew of 761 ns for Fault 2.

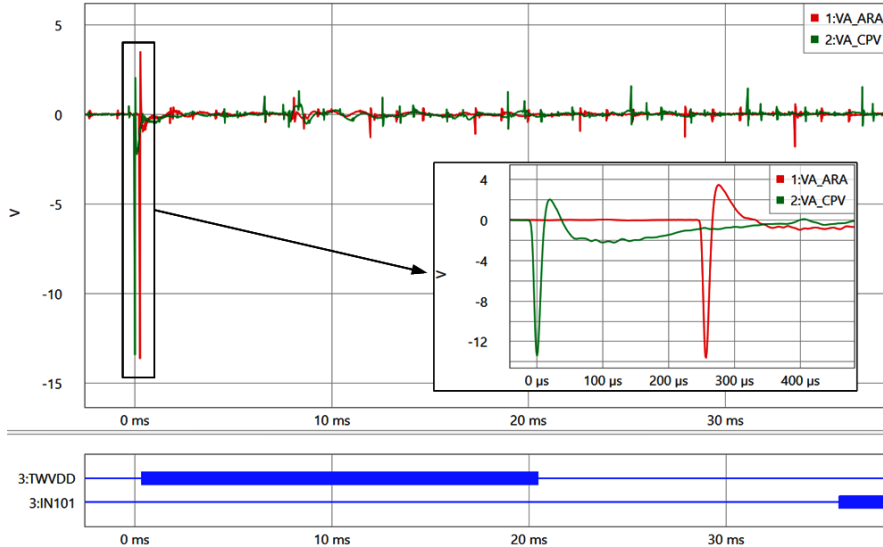


Fig. 18. Record of the initial TWs that arrived at each HVdc line terminal and the assertion of TWVDD and IN101 at the local substation for Fault 2.

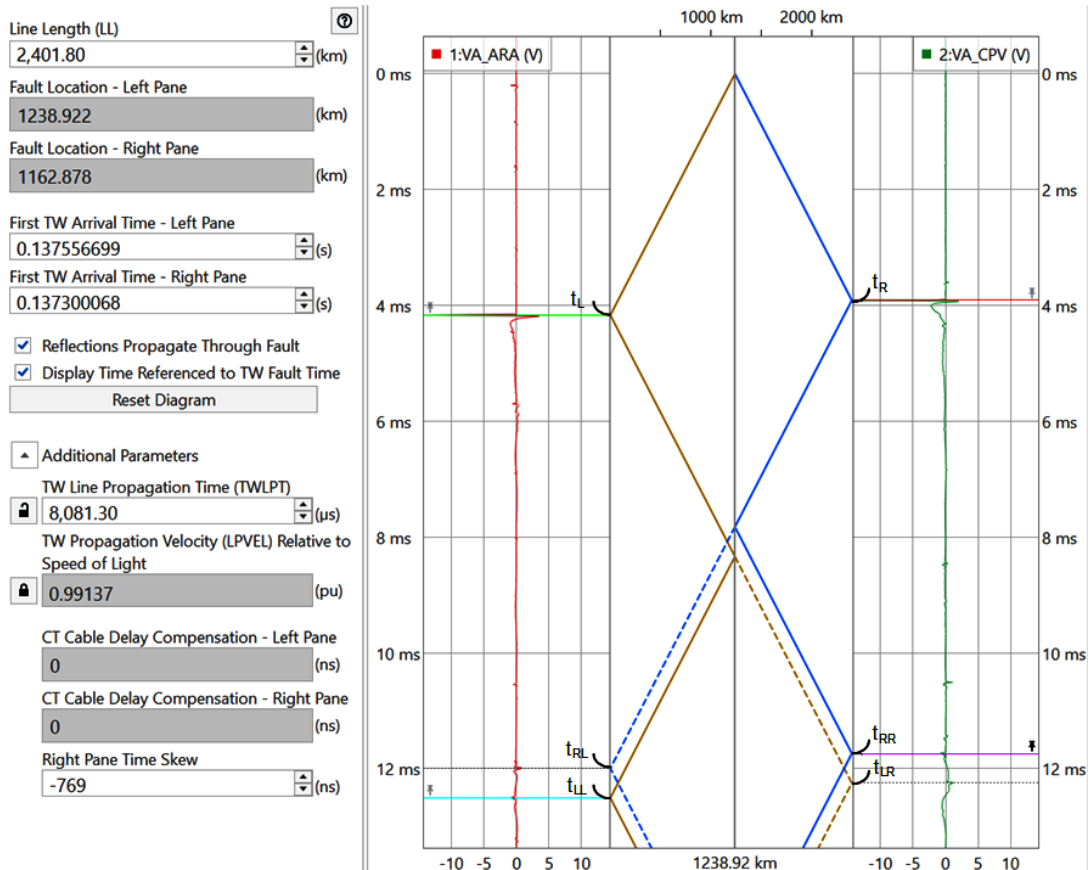


Fig. 19. A Bewley diagram and DETWFL result obtained by using four TW arrival times (t_L , t_R , t_{LL} and t_{RR}) for improved fault location for Fault 2.

B. Offline Fault Location Using Field Records from Staged Faults

With the aim to validate the pilot TWFL project system, staged faults were conducted in the ± 600 kV HVdc Bipole 2 transmission line. Records from UHS relays at each line terminal were used to calculate the fault location following the same procedure as for the actual faults.

Fig. 20, Fig. 21, and Fig. 22 show the Bewley diagrams for staged Fault 1, Fault 2, and Fault 3, respectively. Table I summarizes the fault location results for the pilot TWFL system and the existing LFL. The actual fault location is also shown to calculate the error for each system.

Table I shows that the pilot TWFL system presented fault location accuracy with errors less than 350 m in the HVdc line. These results validate the application, as was the intended goal of the staged fault tests.

TABLE I
SUMMARY OF FAULT LOCATIONS FOR STAGED FAULTS

Staged fault	Actual fault location (km)*	Pilot TWFL system		LFL	
		Fault location (km)*	Error (m)	Fault location (km)*	Error (m)
1	663.822	664.162†	340	662.8	1,022
2	1,124.854	1,124.818†	36	1,124.8	54
3	1,505.431	1,505.229†	202	1,506.3	869

*Fault location results shown are from the Araraquara Station.

†DETWFL using a Bewley diagram with four TW arrival times.

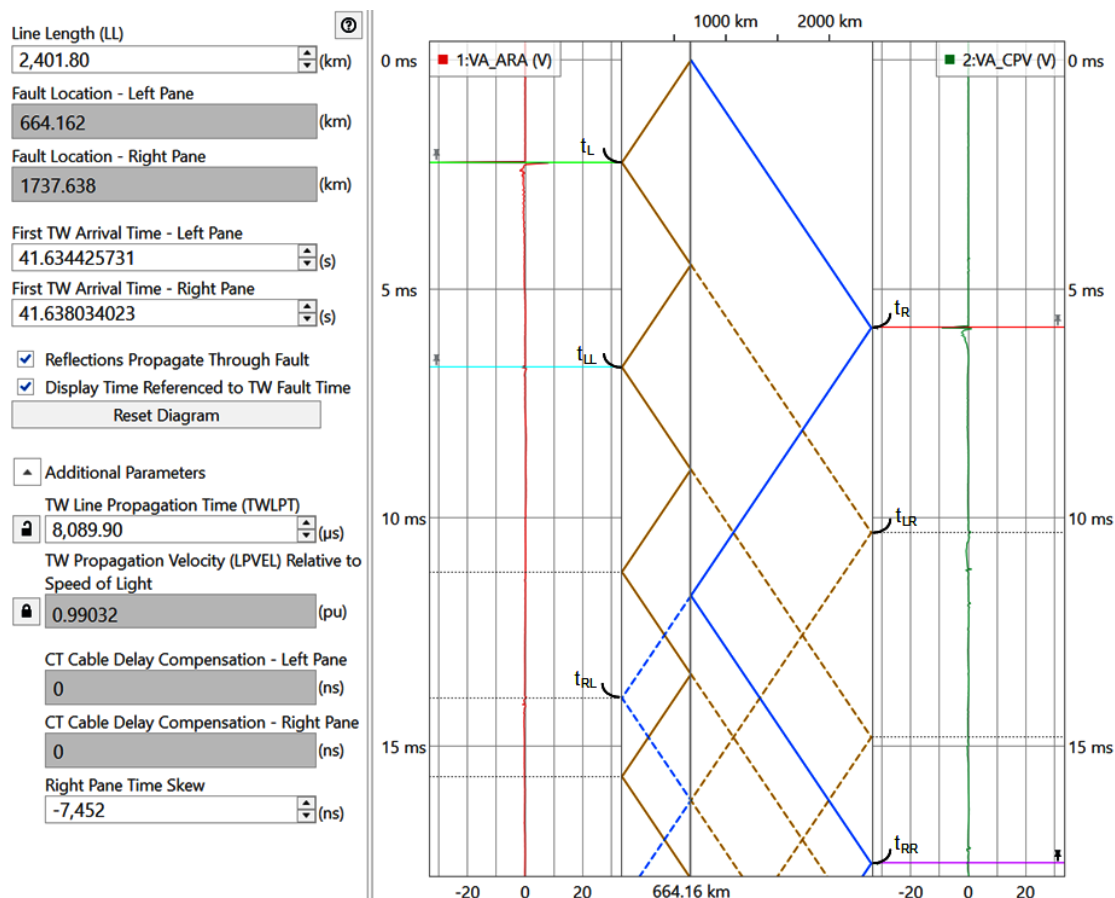


Fig. 20. The Bewley diagram and DETWFL result obtained by using four TW arrival times (t_L , t_R , t_{LL} and t_{RR}) for improved fault location for Staged Fault 1

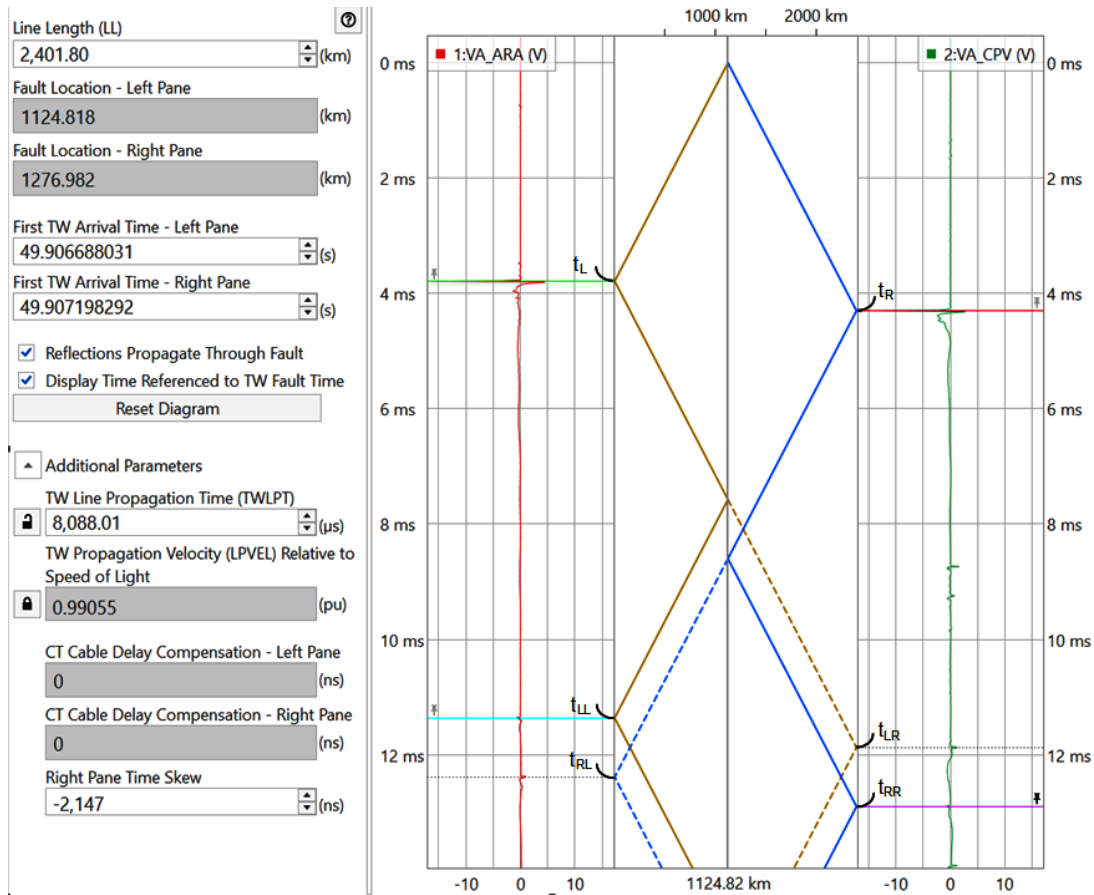


Fig. 21. The Bewley diagram and DETWFL result obtained by using four TW arrival times (t_L , t_R , t_{LL} and t_{RR}) for improved fault location for Staged Fault 2.

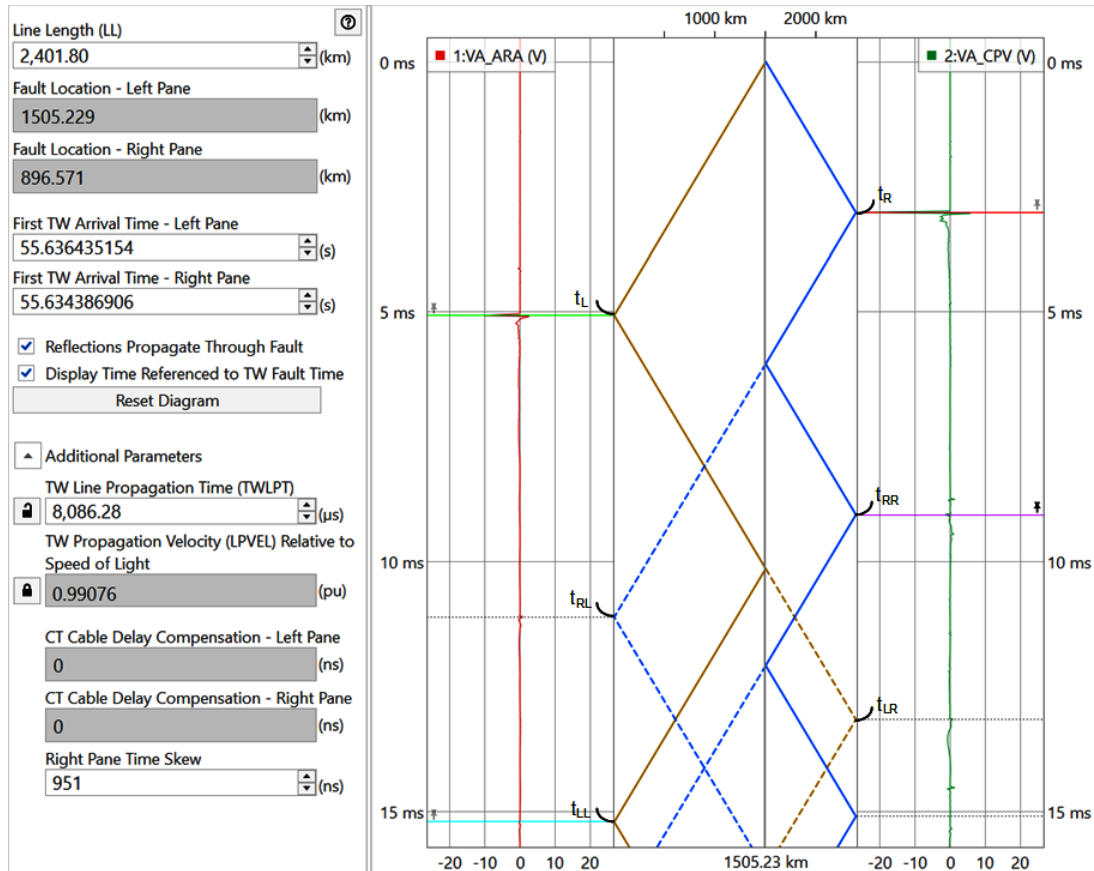


Fig. 22. The Bewley diagram and DETWFL result obtained by using four TW arrival times (t_L , t_R , t_{LL} and t_{RR}) for improved fault location for Staged Fault 3.

C. Low-Energy Events in the HVdc Line

The possibility of detecting and recording transient events using TWVDD instead of the HVdc protection system trigger gives more flexibility to the system and allows the detection of low-energy transients not related to a fault, as fault precursors presented in [10].

Additionally, the smoothing reactors and 500/258 kV power transformers at each HVdc terminal shown in Fig. 1 represent a high-impedance path for TW signals from the ac system, acting as a natural block for external high-frequency events. Since the pilot project was operating, external events to the HVdc line were not recorded.

Several low-energy events were registered during the pilot project. Fig. 23 shows the first TWs that arrived at each terminal for one of these low-energy events, which activated the TWVDD. The TW recorded at time zero is VA_CPV. Fig. 24 shows the Bewley diagram with the result of the DETWFL calculation. Section VI discusses how an automated system logs this information and alerts the users if recurring low-energy events are triggered at the same location.

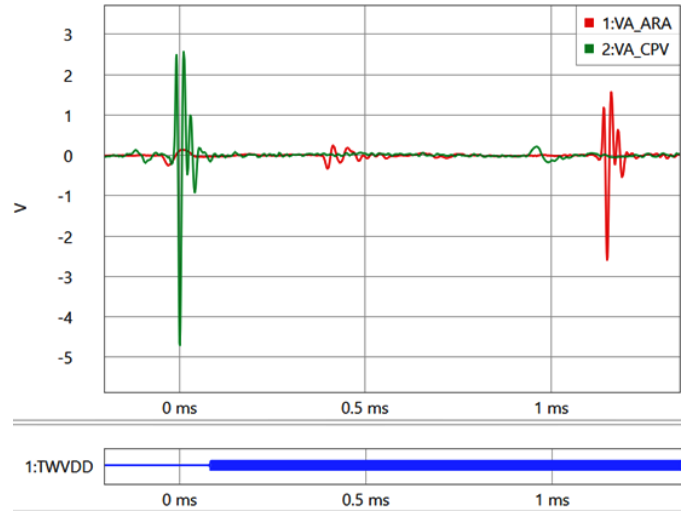


Fig. 23. The first TWs that arrived at each line terminal for the low-energy event.

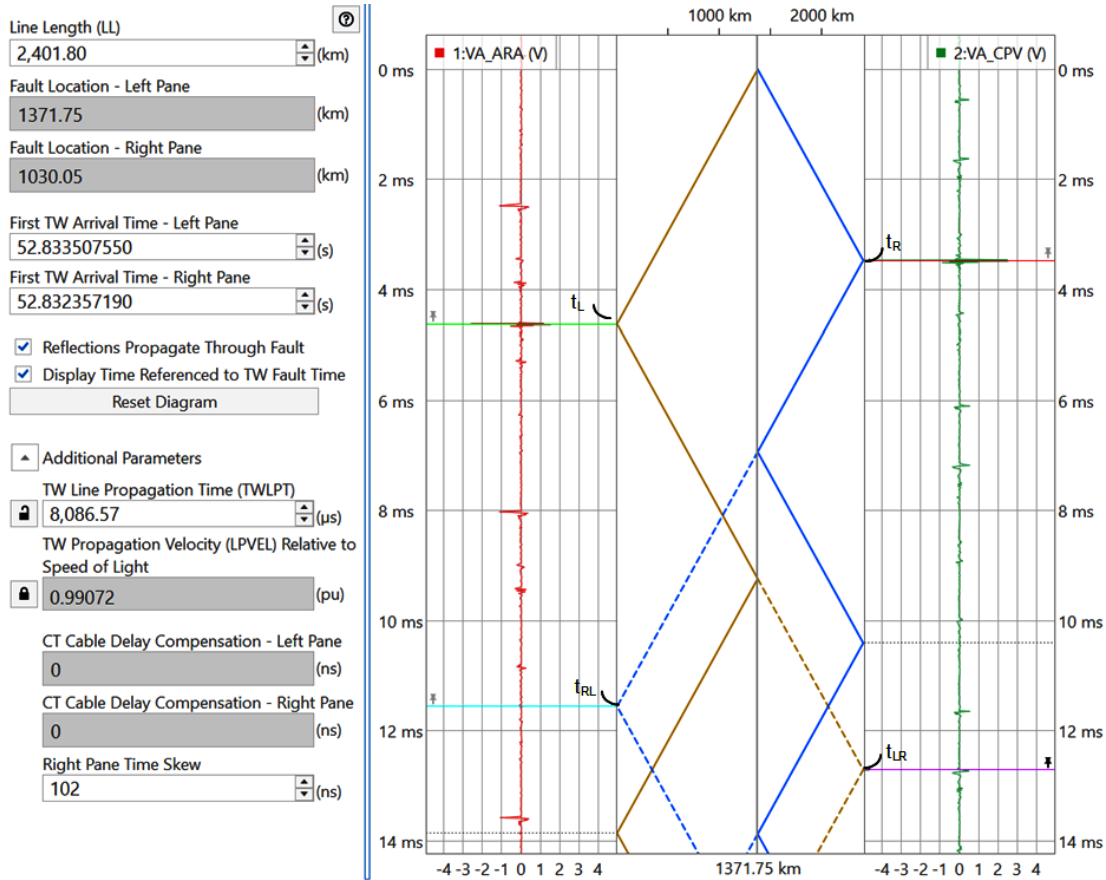


Fig. 24. The Bewley diagram and DETWFL for the low-energy event.

VI. PROVIDING AUTOMATIC FAULT AND LOW-ENERGY EVENT LOCATIONS

This section presents an automatic system for the HVdc TWFL calculation using a real-time automation controller (RTAC) capable of parsing IEEE COMTRADE files from UHS relays. The automatic TW fault location calculation system is illustrated in Fig. 25. The IE Madeira Ethernet backbone allows the RTAC located at the local substation to have an Ethernet connection to the UHS relays in both terminals.

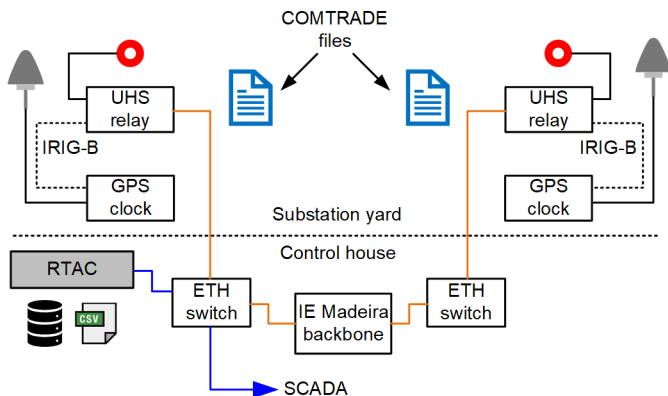


Fig. 25. The automatic TW fault location system.

The automatic fault location calculation is performed according to the following steps:

1. When there is a fault or low-energy event in the HVdc line, the UHS relays at each line terminal trigger high-resolution transient records and notify the RTAC that a new event record is available.
2. The RTAC starts the collection of the high-resolution transient records from both relays and stores them in its database.
3. When event records from both relays are available, the RTAC parses the IEEE COMTRADE files. The time stamp of the first TW that arrived at each terminal is obtained for the fault location calculation.
4. The RTAC applies (1) to estimate the fault location by using the DETWFL method.

The RTAC automatically reports the DETWFL result to the SCADA system over a client/server protocol—DNP3 and IEC 61850 MMS are two of the protocols available. Additionally, the RTAC populates a CSV file with the fault location result and includes the event time stamp, event classification, and status of the fault location. Fig. 26 shows the information contained in the CSV file.

Time Stamp	ARA FL [km]	CPV FL [km]	Location_Type	TW_Time_ARA	TW_Time_CPV	Status
DT#2022-03-30-18:10:52.833600	1371.831	1209.969	EVENT_LOCATION	DT#2022-03-30-18:10:52.833508	DT#2022-03-30-18:10:52.832358	OK
DT#2022-11-09-11:02:41.634500	664.623	1737.176	FAULT_LOCATION	DT#2022-11-09-11:02:41.634426	DT#2022-11-09-11:02:41.638034	OK
DT#2022-11-09-11:02:49.906700	1125.096	1276.704	FAULT_LOCATION	DT#2022-11-09-11:14:49.906688	DT#2022-11-09-11:14:49.907198	OK
DT#2022-11-09-11:48:55.636500	1505.305	896.494	FAULT_LOCATION	DT#2022-11-09-11:48:55.636435	DT#2022-11-09-11:48:55.634387	OK
DT#2023-06-18-04:47:00.137644	1239.099	1162.701	FAULT_LOCATION	DT#2023-06-18-04:47:00.137557	DT#2023-06-18-04:47:00.137300	OK

Fig. 26. The CSV file with fault location information from the RTAC.

Event classification is indicated in the Location_Type field and is classified as Fault_Location when the digital input from the HVdc protection system is asserted (IN101) and TWVDD is asserted. It is categorized as Event_Location when only the TWVDD is asserted.

The status of the fault location is indicated in the Status field and is categorized as OK when all the requirements for the fault location calculation are satisfied. If not, a message relating to the inconsistency is shown. The program performs several checks, including but not limited to:

- High-resolution transient records are available from both line terminals.
- Both UHS relays are time synchronized with high accuracy (error $\leq 1 \mu\text{s}$).
- The difference between the first TWs that arrive at each terminal is less than $\text{TWLPT} + 10 \mu\text{s}$.

Following are the settings required for the automatic TWFL system.

- TWLPT (μs)
- LL (mi or km)
- Local terminal device name
- Remote terminal device name
- Local IEEE COMTRADE file VA channel ID
- Remote IEEE COMTRADE file VA channel ID

To validate the automatic TWFL system, transient records captured during the staged fault tests are played back to the UHS relays that are communicating to the RTAC, using the built-in event playback feature [1] [2]. Table II shows the fault location obtained from the automatic TWFL system for the staged faults. Results are compared with the actual fault location and with the DETWFL estimated using the Bewley diagram tool. LL = 2,401.8 km and TWLPT = 8,079.5 μs are the settings for the results shown in Table II. Results from the Bewley tool and the automated system are comparable—IE Madeira engineers opted for the automated system for operational efficiency.

TABLE II
SUMMARY OF AUTOMATIC FAULT LOCATION RESULTS FOR STAGED FAULTS

Staged fault	Actual fault location (km)*	TWFL using Bewley tool		TWFL using automated system	
		Fault location (km)*	Error (m)	Fault location (km)*	Error (m)
1	663.822	664.162†	340	664.623‡	801
2	1,124.854	1,124.818†	36	1,125.096‡	242
3	1,505.431	1,505.229†	202	1,505.305‡	126

*Fault location results shown are from the Araraquara Station.

†DETWFL using a Bewley diagram with four TW arrival times.

‡DETWFL using the time stamp of the first TWs at each terminal.

VII. CONCLUSIONS

A highly accurate and real-time fault-locating system is an essential tool for TGCs. Such a system provides ways to detect failures in transmission lines in a timely manner to speed up restoration, thereby reducing the costs of line inspections and improving line crew maintenance productivity. An important feature required in a fault-locating system is the ability to record high-resolution oscillography data related to an event, which allows better visibility and understanding of line outage causes and the possibility of performing fault-locating analysis manually in case of a failure of the automated system. Additionally, this system reduces the duration of unexpected line outages, resulting in fewer penalties to the TGCs and improved quality of service to energy consumers.

In this paper, we have shown that a TWFL device originally designed for ac systems can be successfully applied in an HVdc transmission line. Staged faults were conducted, and the data obtained were used to validate the proposed solution, which presented exceptional performance for locating faults in the HVdc line.

The TWFL system proposed in the pilot project provides high-resolution event records, allowing postoperation analysis and fine tuning of a fault location using the Bewley diagram tool. This capability addresses one of the main weaknesses of the LFL system currently in service.

UHS relays with disturbance-detection capability allow the detection and recording of low-energy events that are not related to faults in the HVdc transmission line. Low-energy event location provides continuous monitoring of the HVdc transmission line, which has the potential of reducing the number of line faults and unexpected line outages by indicating the location where repetitive fault precursors occur. This allows the line maintenance crew to fix the problem before a fault occurs.

An automatic fault and low-energy event locating system was presented. This system automatically reports the DETWFL result to the utility control center and provides a CSV file containing the fault and event location historical data.

VIII. REFERENCES

- [1] *SEL-T400L Ultra-High-Speed Transmission Line Relay, Traveling-Wave Fault Locator, High-Resolution Event Recorder Instruction Manual*. Available: selinc.com.
- [2] *SEL-T401L Ultra-High-Speed Line Relay Instruction Manual*. Available: selinc.com.
- [3] E. O. Schweitzer, III, B. Kasztenny, and V. Mynam, "Performance of Time-Domain Line Protection Elements on Real-World Faults," originally presented at the 42nd Annual Western Protective Relay Conference, October 2015.
- [4] S. Marx, B. K. Johnson, A. Guzmán, V. Skendzic, and V. Mynam, "Traveling Wave Fault Location in Protective Relays: Design, Testing, and Results," proceedings of the 16th Annual Georgia Tech Fault and Disturbance Analysis Conference, Atlanta, Georgia, May 2013.
- [5] E. O. Schweitzer, III, A. Guzmán, V. Mynam, V. Skendzic, B. Kasztenny, and S. Marx, "Locating Faults by the Traveling Waves They Launch," originally presented at the 40th Annual Western Protective Relay Conference, October 2013.
- [6] D. López Cortón, J. Vaquero Melado, J. Cruz, R. Kirby, Y. Zafer Korkmaz, G. Patti, and G. Smelich, "Double-Ended Traveling-Wave Fault Locating Without Relay-to-Relay Communications," originally

presented at the 74th Annual Conference for Protective Relay Engineers, March 2021.

- [7] A. Guzmán, B. Kasztenny, Y. Tong, and M. V. Mynam, "Accurate Single-End Fault Locating Using Traveling-Wave Reflection Information," 14th International Conference on Developments in Power System Protection, Belfast, United Kingdom, March 2018.
- [8] S. Marx, E. Blood, and G. Smelich, "Correlating Traveling-Wave Arrival Times to the Bewley Diagram—A New Systematic Approach for Offline Traveling-Wave Fault Locating," originally presented at the 49th Annual Western Protective Relay Conference, October 2022.
- [9] *SEL-T4287 Traveling-Wave Test System Instruction Manual*. Available: selinc.com.
- [10] B. Kasztenny, M. V. Mynam, T. Joshi, and D. Holmbo, "Preventing Line Faults With Continuous Monitoring Based on Current Traveling Waves," presented at the 15th International Conference on Developments in Power System Protection, Liverpool, United Kingdom, March 2020.

IX. BIOGRAPHIES

Diogo Totti Custodio was born in São Gonçalo do Sapucaí—MG, in 1982. He received his BSc and MSc in electrical engineering from the Pontifical Catholic University of Minas Gerais in 2005 and from the State University of Campinas (Unicamp) in 2009, respectively. He worked at SIEMENS as a power systems protection engineer between 2009 and 2014. From 2014 to 2019, he has been working at Interligação Elétrica do Madeira S.A. as a specialist engineer in HVdc protection and control systems and, since 2019, he holds the position of engineering manager in this same company.

Samuel Marques dos Santos Nassif Lacerda was born in Pompéu—MG, in 1983. He received his BSc in electronic engineering from the Pontifical Catholic University of Minas Gerais in 2009. He worked at PROCESS Protection and Control as a SCADA designer specialist. In 2015, he joined GE Service Brazil as field engineer for HVdc systems. In 2016, he joined Interligação Elétrica do Madeira S.A. as a maintenance engineer for HVdc protection and control systems.

Paulo Lima received his BSEE in electrical engineering from Universidade Federal de Itajubá, Brazil, in 2012. In 2013, he joined Schweitzer Engineering Laboratories, Inc. (SEL) as a protection application engineer in Brazil. In 2018, he became application engineering group coordinator and has been the regional technical manager for Brazil since 2020. He has experience in application, training, integration, and testing of digital protective relays. He also provides technical writing and training associated with SEL products and SEL University.

Venkat Mynam received his MSEE from the University of Idaho in 2003 and his BE in electrical and electronics engineering from Andhra University College of Engineering, India, in 2000. He joined Schweitzer Engineering Laboratories, Inc. (SEL) in 2003 as an associate protection engineer in the engineering services division. He is presently working as an engineering director in SEL research and development. He was selected to participate in the U. S. National Academy of Engineering (NAE) 15th Annual U. S. Frontiers of Engineering Symposium. He is a senior member of IEEE and holds patents in the areas of power system protection, control, and fault location.

Ricardo Abboud received his BSEE degree in electrical engineering from Universidade Federal de Uberlândia, Brazil, in 1992. In 1993, he joined CPFL Energia as a protection engineer. In 2000, he joined Schweitzer Engineering Laboratories, Inc. (SEL) as a field application engineer in Brazil, assisting customers in substation protection and automation. In 2005, he became the field engineering manager, and in 2014, he became the engineering services manager. In 2016, he transferred to the SEL headquarters in Pullman as an international technical manager. In 2019, he joined SEL University as a professor, and he is currently a fellow engineer with SEL Engineering Services, Inc. (SEL ES).